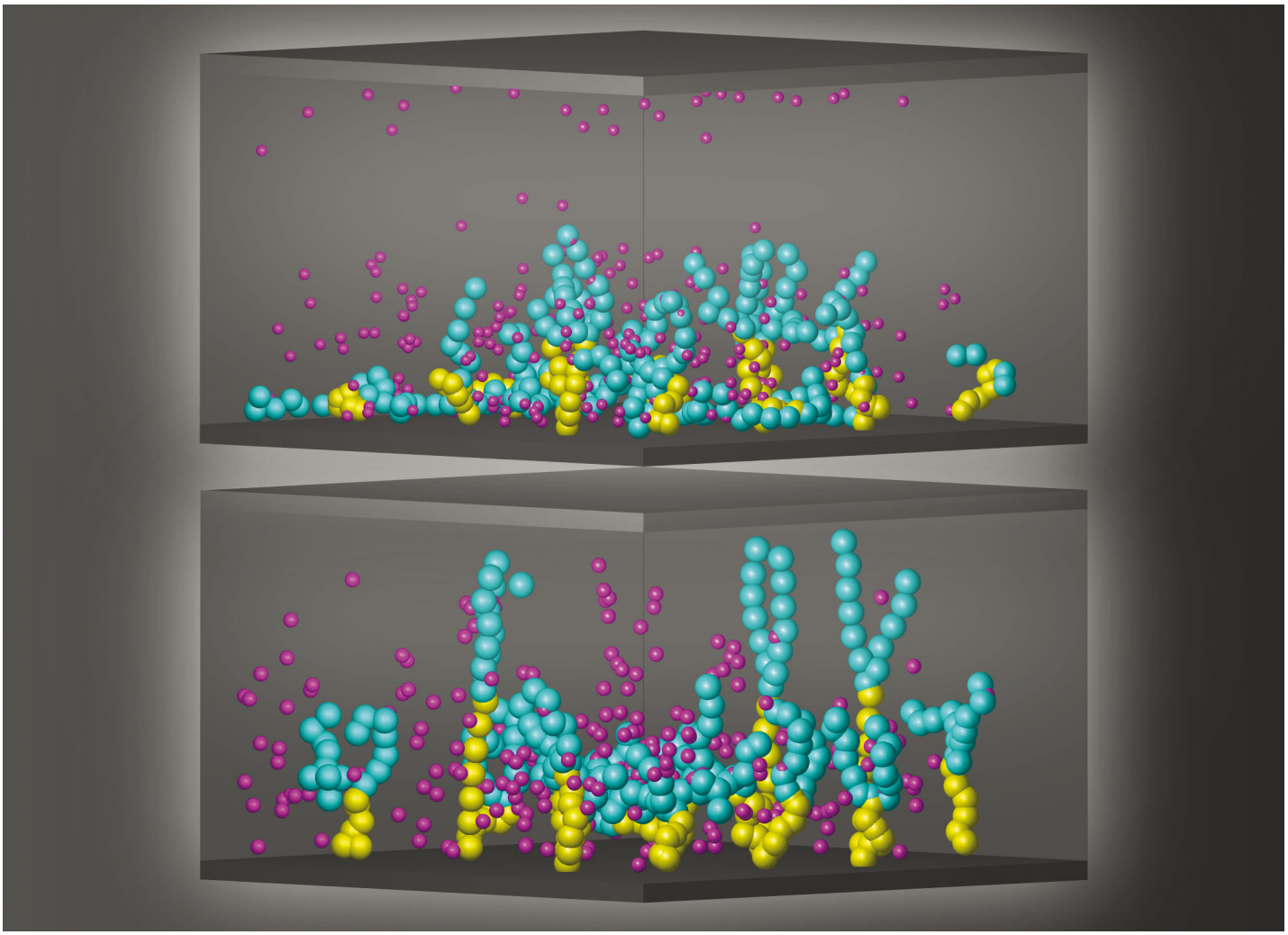

Highlighting research from the group of Prof. Chaohui Tong at the Department of Physics, Ningbo University, China.

Simulations of 3-arm polyelectrolyte star brushes under external electric fields

Branched polyelectrolyte brushes are regarded as exceptionally good candidates for environmental-responsive surface layers. The stretching/collapsing and stratification of 3-arm polyelectrolyte star brushes under external electric fields were studied by Langevin dynamics simulations. An approximate analytical self-consistent field model was also developed to examine the stratification within the brush layer.

As featured in:

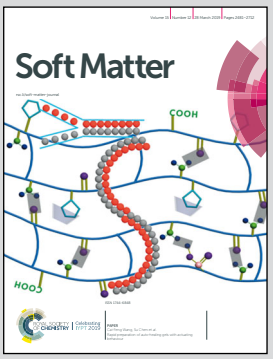

See Chaohui Tong *et al.*, *Soft Matter*, 2019, **15**, 2560.

ROYAL SOCIETY OF CHEMISTRY | Celebrating IYPT 2019

rsc.li/soft-matter-journal

Registered charity number: 207890

Soft Matter

PAPER

View Article Online
View Journal

Cite this: DOI: 10.1039/c8sm02131g

Simulations of 3-arm polyelectrolyte star brushes under external electric fields†

Fen Zhang,[ab] Shaoyun Wang,[a] Huanda Ding[a] and Chaohui Tong *[a]

Langevin dynamics (LD) simulations have been performed to study the conformations and stratification of grafted three-arm polyelectrolyte (PE) stars in response to external electric fields. The grafted chains with neutral stems and fully charged branches were immersed in a salt-free solution sandwiched between the grafting electrode and a second oppositely charged electrode. The branching points of neutral-stem PE brushes at low grafting densities exhibit a bimodal distribution normal to the grafting electrode. With increasing grafting density, the molecular conformations in the brush layer become more complex with the emergence of multi-mode distributions of the branching point monomers. Under strong electric fields, the fraction of grafted chains with either nearly completely stretched stems or collapsed branches onto the grafting electrode gradually decreases with increasing grafting density due to the stronger electrostatic screening from counterions and monomer charges at higher grafting densities. Simulation results revealed that a collapsing electric field promotes the stratification within the brush layer, leading to high degrees of charge overcompensation from charged monomers collapsed onto the oppositely charged grafting electrode. An approximate analytical self-consistent field model was developed to examine the stratification within the brush layer. Regarding the fraction of grafted chains with the free branches in the upper layer, the prediction of the analytical model qualitatively agrees with the simulation results.

Received 19th October 2018,
Accepted 16th January 2019

DOI: 10.1039/c8sm02131g

rsc.li/soft-matter-journal

I. Introduction

Polymer brushes formed by densely end-grafting polymer chains onto solid substrates have been intensively studied in the past few decades due to their scientific and technological importance. Control of wetting properties, colloid stabilization, prevention of nonspecific binding of biomolecules, and acting as stimuli-responsive layers in microfluidics are examples of successful applications of polymer brushes.[1–4] Main research effort has been devoted to polymer brushes made of linear chains and a relatively good physical understanding of linear polymer brushes has been obtained, especially for neutral linear polymer brushes.[5–17] In the last decade, polymer brushes made of branched chains, *e.g.*, dendrimers, have attracted great attention and become the new focus in the research of polymer brushes.[18–31] Compared with linear polymer brushes, branched polymer brushes could mediate the interactions between surfaces in an architecture-dependent manner and lead to improved physical/chemical properties of modified substrates.[23,24] Branched polymer brushes feature a huge number of end groups on the surface of the brushes which could be functionalized. Thus, they are regarded as exceptionally good candidates for environmental-responsive surface layers. Branched polymer brushes are more resistant to interpenetration when pushed to overlap compared with linear brushes and can offer enhanced colloidal stability and tribological properties.[26] Moreover, in some biomedical applications, it is desirable to minimize the overall size of polymer-grafted colloidal particles. Colloidal particles decorated with branched chains can achieve desired colloidal stability with thinner polymer layers.[24]

[a] *Department of Physics, Ningbo University, Ningbo, Zhejiang, 315211, China. E-mail: tongchaohui@nbu.edu.cn*

[b] *Huali College, Guangdong University of Technology, Guangzhou, Guangdong, 511325, China*

† Electronic supplementary information (ESI) available: Methodological details (Section I); snapshot of a row of 3-arm polyelectrolyte brushes under a stretching electric field (Fig. S1), brush center-of-mass height as a function of grafting density at different strengths of the external electric field for the neutral-stem PE brushes (Fig. S2), a comparison of the fraction of grafted chains in the up-state R_{up} and the population weight of grafted chains with their branching points above the mean height H_{bp} in response to external electric fields (Fig. S3), probability distributions of the angle α_{branch} formed by the two vectors connecting the branching point and the two free ends on the branches in each molecule at different strengths of external electric fields (Fig. S4), probability distributions of the angle α_{end} at different strengths of external electric fields (Fig. S5), probability distributions of the free terminal monomers at different strengths of external electric fields at $\sigma_g^* = 0.003$ (Fig. S6), probability distributions of the charged monomers (a) and counterions (b) under different external electric fields for the neutral-stem brushes at low grafting density (Fig. S7); details of the derivation of the analytical self-consistent field theory (Section III), a schematic diagram of the Y-shaped neutral-stem brushes with a two-layered structure adopted in the approximate analytical model (Fig. S8). See DOI: 10.1039/c8sm02131g

In recent years, theoretical and computational studies were conducted to examine the conformational and elastic properties of neutral branched polymer brushes made of dendrons.[23,24] Scaling analysis, analytical mean-field models including self-consistent field (SCF) theory, numerical lattice SCF and molecular dynamics (MD) simulations were employed in these studies.[19–22,25–28] These studies provided insight into the conformational and elastic properties of branched polymer brushes. Two stretching scenarios were proposed in these studies, *i.e.*, the uniform stretching and longest-path stretching. For the uniform stretching scenario, each of the branches of a selected dendron experiences roughly the same amount of stretch. For the longest-path stretching scenario, only a single branch of each generation of a chosen dendron is stretched up, whereas all the other branches remain mostly relaxed. In sharp contrast to mono-disperse brushes made of linear chains, branched brushes consist of molecules with qualitatively different conformations, leading to the emergence of stratification in branched polymer brushes which has been confirmed by lattice SCF and MD simulations. [20,22,27,28] The molecules in branched brushes extend differently in the direction normal to the grafting substrate with a certain fraction of molecules retracting into a collapsed state rather than backfolding. Stratification is characterised by bimodal or multimodal probability distributions of terminal free ends and branching points. Merlitz *et al.* examined the stratification of starlike polymer brushes and accurately predicted the brush height by using a dual phase box-like mean field model which incorporates the finite extensibility of bonds and the hard sphere excluded volume interaction.[22,28] Zhulina and coworkers developed an analytical SCF model to predict the stratification of starlike polymer brushes in the nonlinear elasticity regime.[25] Apart from predicting the brush height, this model can deliver polymer density profiles. The analytical predictions were compared with the results of the numerical lattice SCF model and good agreement between these two models was found.

Up to now, the theoretical and computational studies of branched polymer brushes have focused on neutral brushes, and there is very limited research on ionic (charged) branched brushes. The long-range nature of Coulomb interactions in charged branched brush systems poses great theoretical and computational challenges. The conformational and elastic properties of charged branched brushes are far less understood than neutral branched brushes. Borisov and Zhulina proposed an analytical framework to describe ionic branched brushes made of dendrons.[29] A box-like scaling analysis taking into account the finite extensibility of charged dendrons was developed to predict the brush height. They further presented a self-consistent field framework combined with Poisson–Boltzmann theory to study the internal structure of ionic branched brushes. Furthermore, phase diagrams for starlike charged branched brushes in salt-free and salt-added solutions were constructed. However, in their study, the stratification in charged branched brushes was not considered. Using Monte Carlo simulations, Klos and Sommer studied the collapse of a single charged dendrimer grafted onto one of the electrodes of a planar capacitor.[30] It was found that at low temperature and without an external electric field, the dendrimer is in the osmotic brush regime and nearly all of the counterions are trapped inside the dendrimer. Increasing the strength of the external electric field, counterions are gradually removed from the interior of the dendrimer and accumulate near the opposite electrode. Near a threshold value of electric displacement field, a rather sharp collapse of the dendrimer perpendicular to the grafting electrode was observed. It would be very interesting to see how a truly ionic branched brush instead of a single grafted dendrimer responds to external electric fields, which is nonetheless very expensive computationally. By conducting intensive MD simulations, Miliou and coworkers studied brushes formed by charged star polymers under the theta solvent conditions.[31] Phase diagrams characterizing different brush regimes for salt-free solutions were constructed, which qualitatively agree with those predicted by Borisov and Zhulina. Simulation results of the scaling laws of brush height fully supported the theoretical predictions for the scaling exponents except for the star chain functionality exponent. The internal stratification in the charged starlike brushes was only briefly discussed.

In this work, by performing Langevin Dynamics simulations, we study the stratification of grafted three-arm polyelectrolyte stars (Y-shaped brushes), which have the simplest architecture in branched brushes, and their response to external electric fields applied normal to the grafting electrode. In the Y-shaped brushes, the two branches in each molecule are fully charged, whereas the stem is neutral. The chain conformations and stratification within the brush layer in response to external electric fields were carefully examined. An approximate analytical self-consistent field model similar to that proposed by Zhulina *et al.* for grafted neutral polymer stars,[25] which also incorporates Poisson–Boltzmann theory, was developed to study the stratification within the brush layer in this work.

II. Model and method

In this study, the star-polymer brush system was created as an ensemble of $M = 8 \times 8$ flexible star-polymer chains grafted onto a square lattice with dimensions $L_x \times L_y$ (xy plane) situated at $z = 0$, which was modeled as an impenetrable wall. A corresponding wall at $z = L_z$ closes the system, while periodic boundary conditions were applied only in the x- and y-directions. The grafting density of the star-polymer brush is given by $\sigma_g = M/(L_xL_y)$. Each grafted chain is composed of 3 arms of equal length attached to a central core modeled as a neutral monomer. Each arm consists of 45 monomer units. All of the monomers in the stem (the arm with its end monomer grafted onto the wall at $z = 0$) were assumed to be neutral to further reduce computational effort, and all of the monomers in the other two arms of the same molecule (branches) are charged with charge valence of $q(q = -1)$. Each negatively charged monomer in the branches releases one monovalent counterion into the salt-free aqueous solution sandwiched between the two walls. Water was treated as a uniform dielectric background in

Langevin Dynamics simulations with a dielectric constant of 78 at room temperature. The polymer chains were created by a coarse-grained bead-spring model. Monomers and counterions were modeled as spherical Lennard-Jones (LJ) beads (σ,ε) with equal mass m and diameter σ. The connectivity between two neighboring monomers in the same polymer chain is maintained by the finitely extensible nonlinear elastic (FENE) bond potential. An external electric field $\vec{E}$ was applied perpendicular to the two parallel walls which exerts an electric force $eq\vec{E}$ on a charged particle (e stands for elementary charge and q = +1 for counterions). It should be noted that the electric field applied in LD simulations is equivalent to the electric field generated by the uniform and opposite surface charges on the two walls (a planar capacitor). However, the surface charges on the two walls were excluded from simulations in order to avoid double counting.

All particles interact with each other through a truncated and shifted Lennard-Jones (LJ) potential. With such a purely repulsive interaction between particles in an implicit solvent model, the grafted chains were thus assumed to be immersed in a good solvent. Because the main focus of this work is on the electrostatic interaction in the brush system under external electric fields, the hydrophobic effect of neutral monomers was not considered. Both walls were modeled by a 12/6 Lennard-Jones wall potential. The long-range Coulomb interaction was calculated using the Smooth Particle Mesh Ewald method (SPME) with an approximate root mean square (rms) force error of 10^{-3}.[32] Because the periodic condition is broken in the z direction for the present star-polymer brush system, the Ewald sum was calculated in an extended system which periodically repeats the original slab system in the z direction with the insertion of an empty space whose length is $2 \times L_z$ between them.[33] Furthermore, a correction term was added to the Coulomb potential. The methodological details are provided in Section I of the ESI.†

The time evolution of the system is described by a standard Langevin dynamics. The temperature of the system is $k_BT = 1.2\varepsilon$ with ε denoting the amplitude of LJ potential,[34] and the friction coefficient $\zeta = 1.0m\tau^{-1}$ with the time unit $\tau = \sigma(m/\varepsilon)^{1/2}$.[34,35] Note that such a choice of the system temperature in terms of ε was first used in a pioneering MD simulation work of polymeric systems to prevent polymer chains from crossing.[36] For an aqueous solution at room temperature, Bjerrum length λ_B = 0.71 nm. In this study, we set $\lambda_B = 3\sigma$.[34,35] Thus, $\sigma \approx 0.24$ nm, which is approximately equal to the bond length of polystyrene sulfonate (PSS).[37] Nevertheless, to model fully charged PSS, a three-body cosine/delta bending potential between adjoining monomers needs to be employed besides the FENE potential.[38] In this study, for simplicity, the bending potential between adjoining charged monomers was neglected. The LD unit of the external electric field is $\varepsilon/(e\sigma) = k_BT/(1.2e\sigma) \cong 9.0 \times 10^7$ V m^{-1}. In this work, the electric field strength was explored up to $|\vec{E}| = 1.0$ corresponding to 9.0×10^7 V m^{-1}. Therefore, the "external" electrostatic energy $Ee\sigma$ of counterions or charged monomers is comparable to the thermal energy k_BT. It is worth pointing out that the experimental results indicate that on a time scale of 0.01–10 μs the dielectric breakdown of water occurs at a field strength of the order of 1.0×10^8 V m^{-1}.[39] In this work, the dimensionless grafting density $\sigma_g^* \equiv \sigma_g\sigma^2$ was explored from 0.001 up to 0.1. Furthermore, in this study, the vertical distributions of all the monomers $\phi(z)$, branching points (core monomers) $\phi_{bp}(z)$, charged monomers $\phi_{branch}(z)$ and counterions $\phi_{ion}(z)$ were investigated. All these distributions were normalized such that $\int_0^{L_z} P(z)\mathrm{d}z = 1$, where $P(z)$ stands for either $\phi(z)$, $\phi_{bp}(z)$, $\phi_{branch}(z)$ or $\phi_{ion}(z)$.

The positions and velocities of all particles were updated by the Verlet algorithm with an integration time step of $\delta t = 0.005\tau$. It took 5×10^6 time steps to bring the initial system into an equilibrium state, followed by a production run phase. The data for each ensemble were computed by averaging over 2×10^7 time steps, during which a trajectory of 20 000 configurations were stored for the subsequent data analysis. Snapshots of the brush system under external electric fields are shown in Fig. 1 and Fig. S1 in the ESI.†

III. Results and discussions

1. Center-of-mass height of neutral-stem PE brushes

The response of 3-arm PE brushes with neutral stems to external electric fields in terms of the center-of-mass height as a function of the applied electric field is illustrated in Fig. 2. The center of mass height H_{cm} is defined as $H_{cm} = \int_0^{L_z} z\phi(z)\mathrm{d}z \Big/ \int_0^{L_z} \phi(z)\mathrm{d}z$, with $\phi(z)$ denoting the vertical monomer density distribution (see Fig. 3). Taking the brush height in the absence of external electric fields as a reference, the relative change in the brush height at $\sigma_g^* = 0.003$ in the parameter range shown in Fig. 2 is from +47% to −24%. As shown in Fig. 3, under a strongly negative electric field, *i.e.*, $E = -1.0$, there is a long plateau extending up to about 80σ in the vertical monomer distribution of brushes at $\sigma_g^* = 0.003$, suggesting that the Y-shaped PE brushes are significantly

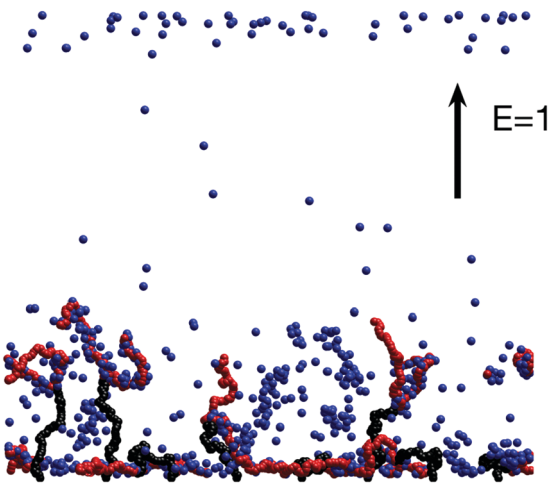

Fig. 1 A snapshot of a row of 3-arm polyelectrolyte brushes under a collapsing electric field (E = 1.0). The blue, red and black spheres represent counterions, charged monomers and neutral monomers, respectively.

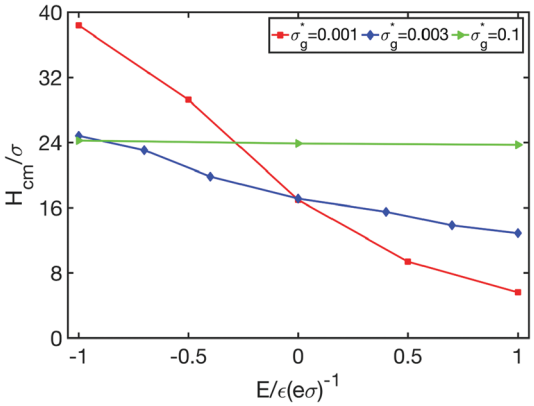

Fig. 2 Brush center-of-mass height as a function of the strength of the external electric field for the neutral-stem PE brushes at different grafting densities. The dimensionless electric field strength of $\varepsilon/e\sigma$ corresponds to 9.0×10^7 V m^{-1}. Note that error bars are of the order of symbol sizes in the figure. In subsequent figures, error bars are only shown in the case that they are much larger than the symbol sizes.

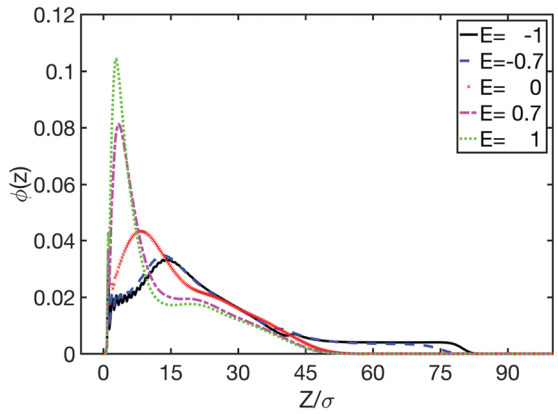

Fig. 3 Vertical monomer density profiles at different external electric fields for the neutral-stem PE brushes at $\sigma_g^* = 0.003$. Note that the vertical monomer density is normalized by the condition of $\int_0^{L_z} \phi(z)\mathrm{d}z = 1$.

stretched because the contour length from the grafting monomer to one of the free end monomers in a polymer chain is about 90σ.

The effect of grafting density on the brush height in response to external electric fields is illustrated in Fig. 2 and Fig. S2 in the ESI.† Clearly, as the grafting density increases, the Y-shaped PE brushes become less responsive to external electric fields. It has been verified that $\sigma_g^* = 0.001$ corresponds to the mushroom regime in which the grafted chains are far apart and isolated from each other. The surface layer formed by the grafted Y-shaped PE chains becomes a brush layer at $\sigma_g^* \approx 0.003$. It was found from simulations that the two-dimensional (2D) radii of gyration parallel to the grafting electrode of isolated grafted Y-shaped chains at $\sigma_g^* = 0.001$ are about 7σ, 8σ and 12σ at $E = -1$, 0, and 1, respectively. Because the lateral size of the simulation box is about 25σ at the highest grafting density of $\sigma_g^* = 0.1$, which is larger than twice the 2D radius of gyration of isolated grafted chains, the finite size effect should be insignificant.

The much reduced sensitivity of the charged Y-shaped brushes to applied electric fields at high grafting densities is due to the stronger electrostatic screening effect from more concentrated charged monomers and counterions. Debye screening length r_D is a measure of the strength of electrostatic screening effect of mobile ions in an electrolyte solution. For the present brush system, taking into account the screening effect of charged monomers, the Debye length can be calculated from the following expression:

$$r_D = (8\pi\lambda_B N_c c_b)^{-1/2} = \left[8\pi\left(\frac{\lambda_B}{\sigma}\right)N_c\frac{\sigma_g^*}{(L_z/\sigma)}\right]^{-1/2}\sigma \qquad (1)$$

where c_b denotes the average number density of grafted Y-shaped polymer chains ($c_b = \sigma_g/L_z$ with $L_z = 130\sigma$ in this study), and N_c is the total number of charged monomers per grafted chain ($N_c = 90$ for the 3-arm PE brushes with neutral stems in this study). The Debye screening length decreases from 4.4σ to 0.44σ when the grafting density increases from $\sigma_g^* = 0.001$ to 0.1. The maximum electric field strength of 9×10^7 V m^{-1} used in this simulation work is in line with the experimental observation.[4,39] Optical ellipsometry and neutron refractivity measurements of the response of linear polyelectrolyte brushes to external electric fields showed that, at high applied voltage bias (electric potential difference between the polyelectrolyte chains anchored electrode and the second electrode), dielectric breakdown of aqueous solution and permanent damage to the brush took place.[4] In this experimental study, the maximum electric field strength is estimated to be on the order of 10^8 V m^{-1}, assuming that the voltage bias of 3 V dropped across the $\sim$25 nm thick brush layer (the separation between the two electrodes is about 3 mm).

2. Probability distribution of the branching points and the stratification of the brush layer for neutral-stem PE brushes

The probability distribution of the branching points is intimately related to chain conformations and the degree of stratification of the Y-shaped PE brushes. We have quantitatively examined the stratification in the Y-shaped brushes. We calculated the fractions of the up- and down-populations in the following way: first, the average vertical coordinate of the branching points of all grafted molecules was evaluated. A molecule having all of the monomers in both branches above the average height of the branching points was subsequently defined to be up. Conversely, a molecule with all of the monomers in both branches below that average height was regarded as down. The remaining subset of grafted molecules was in an intermediate state. The effect of external electric fields on the vertical probability distribution of the branching points of neutral-stem PE brushes with low grafting density is illustrated in Fig. 4. Also, the dependence of the fractions of grafted chains in the up- and down-states on the strength of electric fields is shown in Fig. 5. In the absence of external electric fields, the distribution of branching points of the neutral-stem PE brushes exhibits, to some extent, a bimodal feature with significant overlapping of the two modes. The fraction of branched chains in the down-state is quite small

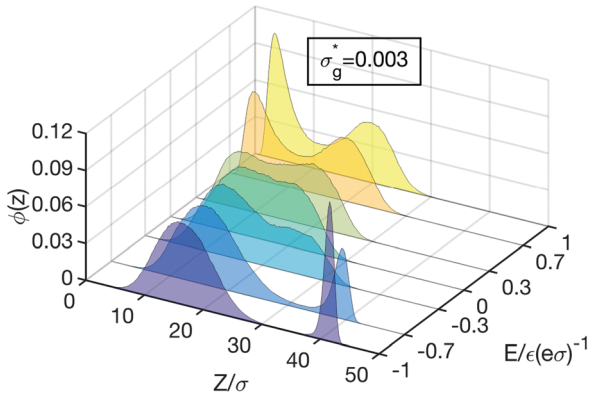

Fig. 4 Probability distributions of the branching point monomers under different external electric fields for the neutral-stem PE brushes at σ_g^* = 0.003.

(~5%, as shown in Fig. 5), whereas the fraction of grafted chains in the up-state is relatively high, *i.e.*, ~33%. Because backfolding of branches towards the grafting substrate is a relatively low probability event for branched brushes, most of the grafted chains with their branching points above the mean height H_{bp} should be in the up-state. From the comparison between R_{up} (the fraction of grafted chains in the up-state) and R_{area} (the population weight of grafted chains with their branching points above the mean height H_{bp} obtained from Fig. 4 and 5) (see Fig. S3 in the ESI† for the comparison), it can be deduced that, at E = 0, about 67% (0.33/0.49, see Fig. S3, ESI†) of the grafted chains with their branching points above the mean height H_{bp} have all of their charged monomers above the mean height H_{bp}, and the rest 33% are in the intermediate state.

For the branched PE brushes with σ_g^* = 0.003 under a negative electric field, accompanied by the stretching of grafted chains, both modes of the distribution of the branching points move to larger heights and are farther apart as shown in Fig. 4. At E = −0.7 and E = −1.0, the two modes become cleanly separated from each other and the peak at larger height becomes higher and narrower as the electric field strength increases. At E = −1.0, the peak positioned at ~40σ clearly indicates that a fraction of neutral stems are almost completely stretched because the contour length of neutral stems is about 45σ. Because all of the grafted chains are stretched to varying degrees under negative external electric fields, the fraction of down-state chains remains small (see Fig. 5). On the other hand, the fraction of chains in the up-state slightly decreases with increasing strength of the negative electric field for E < −0.3 due to the relatively rapid increase of the mean height H_{bp} of all the branching points used to quantify the up- and down-populations. Moreover, as shown in Fig. S3 (ESI†), the strong stretching of the charged branches results in a drastic reduction in the difference between the fraction of chains in the up-state and the population weight of chains with their branching points above the mean height in a strongly negative electric field. Although the combined fraction of molecules in the up- and down-states does not increase in negative electric fields, the contrast between the up- and down-states becomes much sharper in a strongly negative electric field compared to that in the absence of electric fields, as revealed by the well separated modes in the distribution of the branching points at E = −1.0.

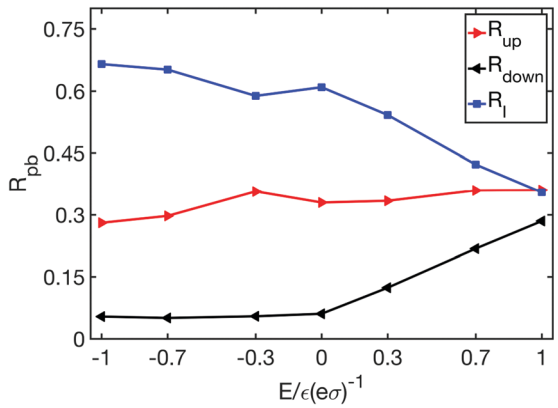

Fig. 5 Fractions of grafted chains in the up-state R_{up}, down-state R_{down} and intermediate-state R_I as a function of the strength of the external electric field for the neutral-stem brushes at a low grafting density of σ_g^* = 0.003.

For neutral-stem PE brushes with σ_g^* = 0.003 under a positive electric field, as the field strength increases, the left mode of the bimodal probability distribution of the branching points shifts towards the grafting electrode and grows at the expense of the other mode. The right mode with larger height also shifts slightly towards the grafting electrode under a positive electric field. Fig. 5 clearly shows that the fraction of grafted chains in the down-state increases quite rapidly with increasing strength of the positive electric field due to the strong electrostatic attraction between charged monomers on the branches and the oppositely charged grafting electrode. It can be further seen from Fig. 5 that the positive external electric field has rather weak influence on the fraction of grafted chains in the up-state. This is because the mean height H_{bp} decreases with increasing strength of positive electric fields, although the population weight of the right mode of the probability distribution of branching points decreases as the field strength is increased. Furthermore, as shown in Fig. S3 (ESI†), the difference between the fraction of up-state molecules and the population weight of molecules with their branching points above the mean height H_{bp} is not affected much by positive electric fields.

The effect of grafting density on the probability distribution of the branching point monomers in response to external electric fields was examined. It can be clearly seen from Fig. 6a and b that, in the brush regime, with increasing grafting density, the molecular conformations become more complex with the emergence of multi-mode distributions of the branching point monomers. Also, due to the stronger electrostatic screening from counterions and monomer charges, the degree of chain stretching or collapsing gradually decreases with increasing grafting density as revealed by the reduced fraction of the strongly stretched branching point monomers with a vertical coordinate of about 40σ.

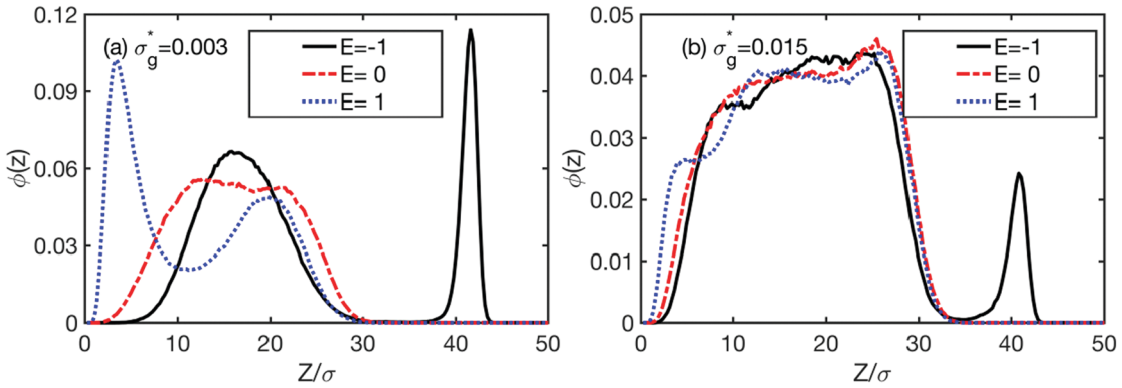

Fig. 6 Vertical probability distributions of the branching point monomers under different external electric fields for the neutral-stem PE brushes at different grafting densities.

3. Probability distributions of the different orientational angles for neutral-stem PE brushes

In order to investigate the chain conformations and morphology of the brush layer more thoroughly, we examined the orientations of both the stem and branches of grafted Y-shaped chains. Three different angles were employed to study the orientations as shown in Fig. 7. The first one is the angle formed by the vector connecting the grafting point and the branch point in each molecule with respect to the grafting substrate and is denoted by α_{stem}. The other two are respectively the angle α_{branch} formed by the two vectors connecting the branching point with the two free ends on the branches of each molecule and the angle α_{end} made by the vector linking the two free ends on the branches of each molecule with respect to the grafting substrate. It is noted that α_{stem} and α_{end} were used to study the morphology of neutral Y-shaped polymer chains grafted onto a planar substrate.[18]

It can be clearly seen from Fig. 8 that, in the absence of external electric fields, the distribution of the angle α_{stem} reaches a maximum probability at $\alpha_{stem} \approx 80^\circ$. Due to the flexible nature of grafted polymer chains and the thermal fluctuation, the most probable angle α_{stem} is smaller than 90°. Under an external electric field of $E = -1$, due to the strong stretching of the grafted chains, the stems become more perpendicular to the grafting substrate compared with the case of $E = 0$, and a large fraction of stems are nearly perpendicular to the grafting substrate. When grafting Y-shaped chains collapse under an external electric field, a bimodal distribution of the angle α_{stem} emerges as shown in Fig. 8. The mode centered at $\alpha_{stem} \approx 19^\circ$ corresponds to the collapsed Y-shaped chains.

As shown in Fig. S4 in the ESI,† the distribution of the angle α_{branch} in the absence of external electric field is quite broad with very low probability weights at angles smaller than $\sim 15^\circ$. This can be attributed to the strong electrostatic repulsion between the two charged branches in the same molecule and the low grafting density. The strong stretching of grafted chains under external electric field of $E = -1$ results in the emergence of a new and relatively sharp peak centered at $\alpha_{branch} \approx 28^\circ$ in the probability distribution of the angle α_{branch}. On the other hand, when grafted chains collapse under an external electric field, the probability distribution shifts slightly to larger angles compared with the case of $E = 0$.

In the absence of external electric fields, the probability weight of the angle α_{end} gradually decreases from 0° to 90° (see Fig. S5 in the ESI†). Please note that $\alpha_{end} = 0^\circ$ corresponds to the situation in

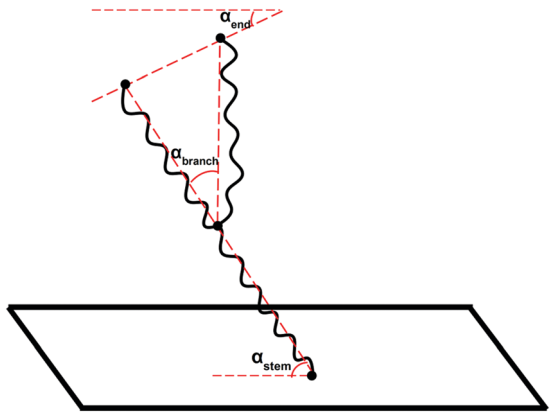

Fig. 7 Schematic representation of the different orientational angles of grafting Y-shaped chains.

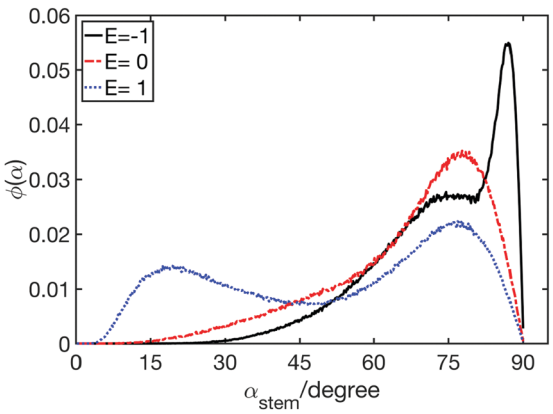

Fig. 8 Probability distributions of the angle α_{stem} formed by the vector connecting the grafting point and the branch point in each molecule with respect to the grafting substrate at different strengths of external electric fields. The grafting density is $\sigma_g^* = 0.003$.

which the two free ends of the branches in the same molecule are at equal vertical distance from the grafting substrate. As shown in Fig. S5 (ESI†), the probability weights of the angle α_{end} at low angles are greatly enhanced by external electric fields and the weight at $\alpha_{end} \approx 0^\circ$ attains a maximum value. The two free ends in each of the strongly stretched chains at $E = -1$ should be of nearly equal height, which contributes to the enhanced probability weight of α_{end} at low angles. On the other hand, the two branches in each of the collapsed chains at $E = 1$ more or less flatten out on the oppositely charged grafting electrode, leading to the two free ends at about the same height. Fig. S5 (ESI†) further shows that the population weight of the angle α_{end} at $\alpha_{end} = 0^\circ$ in the case of $E = 1.0$ is higher than that in the case of $E = -1.0$. This originates from the fact that the fraction of collapsed free end monomers in the immediate vicinity of the grafting electrode is larger than that of strongly stretched free end monomers located at about 80σ as revealed from the probability distributions of the free end monomers (see Fig. S6 in the ESI†). The larger fraction of collapsed free end monomers compared to that of strongly stretched ones is due to the charge overcompensation near the grafting electrode for collapsed Y-shaped PE brushes, which is to be discussed in the next subsection.

4. Probability distributions of charged monomers and counterions and the charge overcompensation near the grafting electrode

The electrostatic interaction plays a vital role in the response of charged polymer brushes to external electric fields. So the probability distributions of the charged monomers and the released counterions were calculated (see Fig. 9 and Fig. S7, ESI†). In the absence of external electric fields, the nearly identical probability distributions of charged monomers and counterions (see Fig. 9) imply that the Y-shaped polyelectrolyte brushes are in the osmotic brush regime. In a positive external electric field, as the field strength increases, the population weight of the charged monomers in the newly emerged mode in the immediate vicinity of the grafting electrode grows at the expense of the original modes (see Fig. 9(a)). In a negative electric field, the charged monomers are repelled from the grafting electrode, leading to the upward shift of the probability distribution of charged monomers away from the grafting electrode as shown in Fig. S7 (ESI†). At $E = -1.0$, a plateau in the range of 50–80σ from the grafting electrode is clearly evident, indicating that the charged branches are strongly stretched. Note that the contour length of a thread from the grafting monomer to either one of the free end monomers is about 90σ.

Upon applying a negative electric field, the positively charged counterions are attracted towards the grafting electrode (see Fig. S1 in the ESI† for a snapshot of a row of the brush system) and a new sharp peak in the counterion distribution emerges in the immediate vicinity of the grafting electrode as shown in Fig. S7(b) (ESI†). Consistent with previous MD simulations of the stretching of linear polyelectrolyte brushes under an external electric field, the counterions enriched near the grafting electrode approximately charge-compensate the opposite charges on the grafting electrode.[34,35,40] Furthermore, Fig. S7(b) (ESI†) clearly shows that a fraction of counterions corresponding to the tail region of the probability distribution profile move to larger height due to the strong electrostatic attraction of charged monomers in the highly stretched branches under strong negative electric fields.

Under a positive electric field, for neutral-stem brushes, Fig. 9(b) and 1 unequivocally show that some counterions accumulate near the grafting electrode despite the fact that the counterions and the surface charges on the grafting electrode are of the same charge sign. Thus, charge overcompensation from collapsed charged monomers on oppositely charged grafting electrode takes place for branched polyelectrolyte brushes. That is, the total number of charges on the collapsed branches exceeds that of the opposite surface charges on the grafting electrode. Nevertheless, including the contributions of both types of charges on the collapsed monomers and counterions, an approximate charge balance near the grafting electrode is maintained under a positive external electric field. Furthermore, as shown in Fig. 5, the fraction of grafted chains in the down-state increases rapidly with increasing strength of positive external electric fields. It should be noted that, for linear polyelectrolyte brushes

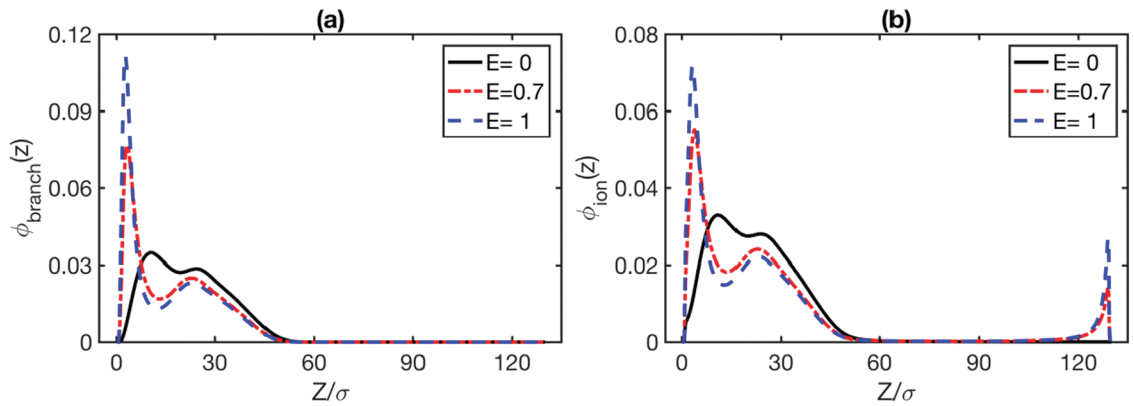

Fig. 9 Probability distributions of the charged monomers (a) and of counterions (b) under different external electric fields for the neutral-stem brushes at low grafting density (σ_g* = 0.003). Note that the probability distribution of counterions is normalized such that $\int_0^{L_z} \phi_{branch}(z)dz = 1$ and $\int_0^{L_z} \phi_{ion}(z)dz = 1$.

collapsing on the grafting electrode, previous MD simulations and SCFT calculations showed that counterions are repelled from the grafting electrode, and no charge overcompensation from collapsed oppositely charged monomers emerges.[40–44] The reason for the absence of charge overcompensation in previous MD simulations is that only very limited parameter space was explored. In particular, the fraction of elementary charge carried by each monomer in MD simulations of ref. 40 is only 1/12, whereas in the present study, each monomer carries one elementary charge. In MD simulations of ref. 42, each monomer carries one elementary charge, but the ratio of the Bjerrum length to monomer diameter, which dictates the range of Coulomb interaction, is much smaller than that in this study, 0.1 *versus* 3. It seems that a large ratio of Bjerrum length to monomer diameter and high charge fraction of monomers would likely lead to charge overcompensation for linear polyelectrolyte chains collapsing under an external electric field.[45] The absence of charge overcompensation in SCFT calculations is due to the fact that SCFT is a mean-field theory, which neglects the charge correlation and charge density fluctuations.

The degree of charge overcompensation Ξ is defined as

$$\Xi = \frac{N_c \beta_I}{s\sigma_e} - 1 = \frac{4.8\pi \cdot (\lambda_B/\sigma) \cdot \sigma_g^* \cdot N_c \cdot \beta_I}{E} - 1 \qquad (2)$$

with s denoting the average surface area occupied by one grafted chain ($s = 1/\sigma_g = \sigma^2/\sigma_g*$), and β_I denoting the weight fraction of the first peak of the normalized probability distribution of charged monomers. In the above equation, σ_e is the surface charge density on the two oppositely charged electrodes ($\sigma_e = \varepsilon_0\varepsilon_r|E|$ in SI unit with ε_0 and ε_r denoting the vacuum permittivity and the dielectric constant of water, respectively). Simulation results further revealed that the degree of charge overcompensation increases with grafting density in the low grafting density regime, but rapidly approaches saturation at relatively high grafting density (see Fig. 10). The increase of the degree of charge overcompensation with grafting density in the low grafting density regime tends to enhance the degree of stratification in the brush layer. The eventual saturation at relatively high grafting density stems from the strong electrostatic repulsion between the collapsed charged monomers.

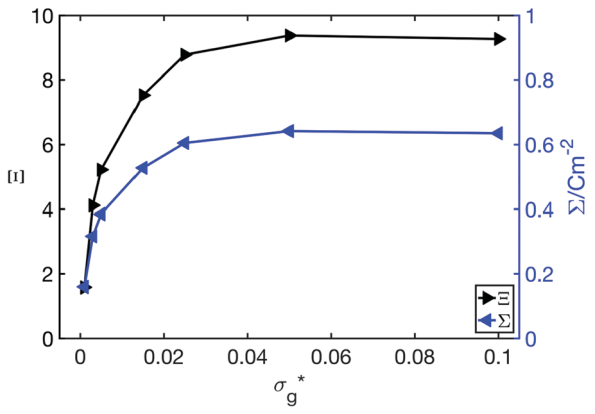

Fig. 10 Degree of charge overcompensation Ξ (black curve) and the net charge of the brush collapsed on the grafting electrode $\Sigma(\Sigma = N_c\beta_I e/s)$ in units of C m^{-2} (blue curve) as a function of grafting density for neutral stem Y-shaped PE brushes at E = 1.0.

In this work, for simplicity, counterions and monomers were assumed to be of equal size. In most cases it is expected that the hydrodynamic radius of ions/counterions should be significantly smaller than monomer units. The equal size assumption might lead to a strong overestimation of the steric effect of counterions in the immediate vicinity of the grafting electrode for collapsed polyelectrolyte brushes. The volume fraction of counterions in the region of z = 0–9σ above the grafting electrode was found to be about 0.04 under a strong collapsing electric field (E = 1.0) for the Y-shaped PE brushes with a grafting density of σ_g^* = 0.1, indicating that charged particles are densely packed near the grafting electrode. It can be expected that if the stems of the Y-shaped brushes are also fully charged like the branches, the steric effect of charged particles near the grafting electrode under a strong collapsing electric field will become more severe. The influence of the steric effect of counterions on the degree of charge overcompensation for PE brushes collapsing under external electric fields will be investigated in the future.

5. Analytical self-consistent field model for the stratification in grafted polyelectrolyte stars

Following the analytical self-consistent field model of grafted neutral polymer stars,[25] the brush layer of grafted polyelectrolyte stars with neutral stems is divided into two sub-layers with thicknesses H_1(lower sub-layer) and H_2(upper sub-layer), respectively (see Fig. S8 in the ESI† for the schematic diagram of the system under consideration). A fraction of stars β have strongly stretched stems with the free branches occupying the upper layer, and the branching points of these stars delineate the boundary between the two sub-layers. The rest of the stars with a fraction of $1 - \beta$ reside in the lower sub-layer and are only weakly stretched. The grafted PE stars with neutral stems are immersed in a salt-free aqueous solution. The molecular potentials acting on the monomers in the two sub-layers are[25]

$$U(z) = \begin{cases} U_1(z), & 0 \le z \le H_1 \\ U_2(z), & H_1 \le z \le H \end{cases} \qquad (3)$$

$$U_1(z) = 3\ln\frac{\cos(kz/2na)}{\cos(kH_1/2na)\cos[\pi(H-H_1)/2na]} \qquad (4)$$

$$U_2(z) = 3\ln\frac{\cos[\pi(z-H_1)/2na]}{\cos[\pi(H-H_1)/2na]} \qquad (5)$$

$$k = 2\arccos\sqrt{(f-1)/f} \qquad (6)$$

In the above equations, n denotes the number of monomers with size a in each of the f branches of a PE star. The molecular potential coincides with the electrostatic energy per charged monomer for strongly dissociating monomers[29]

$$U_1(z) \approx \frac{e\Psi_{in}^I(z)}{k_B T} = \psi_{in}^I(z), \quad 0 \le z \le H_1 \qquad (7)$$

$$U_2(z) \approx \frac{e\Psi_{\text{in}}^{\text{II}}(z)}{k_{\text{B}}T} = \psi_{\text{in}}^{\text{II}}(z), \quad H_1 \le z \le H \tag{8}$$

where $\psi_{\text{in}}^{\text{I}}$ and $\psi_{\text{in}}^{\text{II}}$ are respectively the dimensionless electric potentials within the two sub-layers. For ease of analytical manipulation, each monomer on the free arms is assumed to carry one positive elementary charge. The detailed derivation of the analytical self-consistent equations is provided in Section III of the ESI.† The three equations which allow us to find the thickness of each sub-layer and the fraction of strongly stretched dendrons at a given set of system parameters are listed below

$$\frac{3\pi}{2k}\left[\frac{k}{\pi}\tan(kh_1)+\tan(\pi h_2)\right]^2\frac{[\sin(kh_1)-\sin^3(kh_1)/3]}{\cos^3(kh_1)\cos^3(\pi h_2)}+\frac{k}{\pi}\tan(kh_1) = \zeta(1-\beta)(f-1) \tag{9}$$

$$\frac{3}{2}\left[\frac{k}{\pi}\tan(kh_1)+\tan(\pi h_2)\right]^2\frac{[\sin(\pi h_2)-\sin^3(\pi h_2)/3]}{\cos^3(\pi h_2)}+\tan(\pi h_2) = \beta\zeta(f-1) \tag{10}$$

$$\frac{2}{\pi}\beta\zeta\ln\left[\frac{\tan(k/2)+\tan(kh_1)}{\tan(k/2)-\tan(kh_1)}\right] = \frac{[(k/\pi)\tan(kh_1)+\tan(\pi h_2)]^2}{\cos^3(\pi h_2)} \tag{11}$$

where the dimensionless variables h_1 and h_2 are related to H_1 and H_2 as $h_1 = H_1/(2na)$ and $h_2 = H_2/(2na)$. All of the system parameters are lumped into a single dimensionless parameter ζ on which h_1, h_2 and β depend

$$\zeta = \frac{8}{3}\lambda_{\text{B}}a\sigma_{\text{g}}n^2 \tag{12}$$

The parameter ζ is nearly identical to the same $\zeta(\zeta = 4\sqrt{2/3}\lambda_{\text{B}}a\sigma_{\text{g}}n^2\alpha^{3/2}$ with α denoting the fraction of charge carried by one monomer) by which all equilibrium properties of a linear polyelectrolyte brush are governed.[46] The parameter ζ used by Zhulina and Borisov is the ratio of two characteristic lengths, *i.e.*, the height of a brush in the osmotic brush regime and the Gouy–Chapman length of ions spreading above a planar charged surface.[46]

Eqn (9)–(11) were solved numerically (see Section III of the ESI†). For the charged Y-shaped brushes with neutral stems (f = 3), the dependences of the heights of the two sub-layers and the fraction of grafted chains with strongly stretched stems and the free branches occupying the upper layer on the dimensionless parameter ζ are shown in Fig. 11. For a comparison, by varying the grafting density of the Y-shaped brushes with neutral stems in our simulations, the dependences of the fractions of the grafted chains in the up-, down- and intermediate states on ζ were obtained and are illustrated in Fig. 12. Interestingly, the value of β predicted by the approximate analytical self-consistent field model does not differ much from the fraction of grafted chains in the up-state obtained from simulations. Although it is extremely challenging to develop analytical theory to describe quantitatively the chain conformations of grafted charged stars, as far as the two-layered stratification within the brush layer is concerned, the prediction of the approximate analytical model, to a certain extent, qualitatively agrees with the result from simulations.

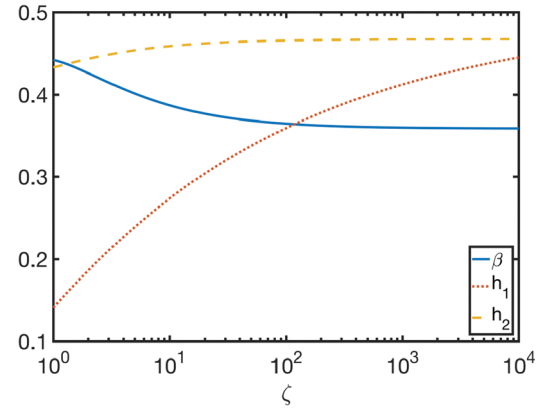

Fig. 11 The dimensionless heights and the fraction of stars with strongly stretched stems and free arms in the upper layer as a function of the dimensionless parameter ζ.

IV. Conclusions

In this work, we have performed Langevin Dynamics simulations to study the conformations and stratification in grafted three-arm polyelectrolyte stars with neutral stems in response to external electric fields. The grafted chains were immersed in a salt-free solution sandwiched between two parallel and oppositely charged electrodes. Compared with linear polyelectrolyte brushes, the chain conformations of grafted polymer stars are more complex with the emergence of stratification within the brush layer.

In the absence of external electric fields, the branching points of neutral-stem Y-shaped PE brushes at low grafting density exhibit a bimodal distribution normal to the grafting

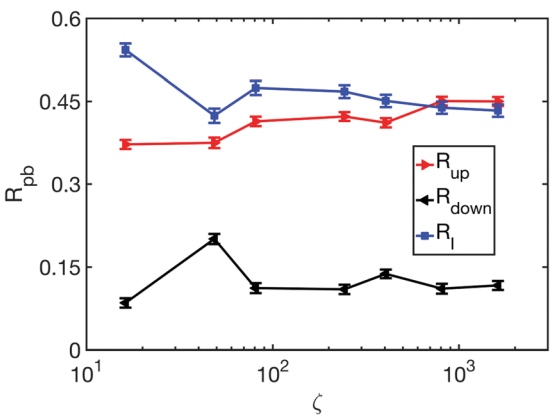

Fig. 12 Fractions of grafted Y-shaped brushes in the up-, down- and intermediate states as a function of the dimensionless parameter ζ obtained from simulations. Note that no external electric field was applied to the brush system.

electrode with significant overlapping of the two modes. In a stretching electric field, both modes of the distribution of the branching points move to increased heights and get farther apart from each other. A fraction of grafted chains are strongly stretched with nearly full extension of the stems. Although the combined fraction of grafted chains in the up- and down-states does not increase under a stretching electric field, the contrast between the up- and down-states becomes much sharper compared to that in the absence of electric fields.

With increasing grafting density, the molecular conformations in the brush layer become more complex with the emergence of multi-mode distributions of the branching point monomers. Also, due to the stronger electrostatic screening from counterions and monomer charges, the fraction of grafted chains with either nearly completely stretched stems or collapsed branches on the grafting electrode gradually decreases with increasing grafting density.

Under a collapsing electric field, the fraction of grafted chains in the down-state increases rapidly with increasing electric field strength. Due to the promotion of stratification in the brush layer by the collapsing electric field, high degrees of charge overcompensation from charged monomers collapsed onto the oppositely charged grafting electrode take place. It should be pointed out that previous MD simulations and SCFT calculations showed that no charge overcompensation takes place for linear polyelectrolyte brushes collapsing under external electric fields.[40–44] Such a different result from that of branched polyelectrolyte brushes revealed in this study is due to the facts that only very limited parameter space was explored in MD simulations of linear polyelectrolyte brushes and SCFT is a mean-field theory. A large ratio of Bjerrum length to monomer diameter, high charge fraction of monomers and/or long chain length in MD simulations would likely lead to charge overcompensation for linear polyelectrolyte brushes collapsing under external electric fields.

An approximate analytical self-consistent field model similar to the one for grafted neutral stars proposed by Zhulina *et al.*,[25] which also incorporates Poisson–Boltzmann theory, was developed to study the stratification of charged star polymer brushes. The model assumes a dual layer structure with sharp boundary within the brush layer and completely neglects the contribution of grafted chains in the intermediate state (parts of the free branches in both the upper and lower layers). As far as the fraction of the grafted chains in the upper layer is concerned, the prediction of the approximate analytical model qualitatively agrees with the simulation result.

Finally, we would like to point out that in this work, we only considered the simplest architecture of branched polyelectrolyte brushes, namely grafted 3-arm stars. Branched PE brushes with higher generations and branching point functionalities were not considered. Nevertheless, this work revealed that the response of Y-shaped PE brushes in terms of chain conformations and stratification to external electric fields is highly nontrivial and qualitatively different from that of linear PE brushes. The response of branched PE brushes with more complex architectures to external electric fields will be the subject of our future work.

Conflicts of interest

There are no conflicts to declare.

Acknowledgements

The authors thank the financial support from the National Natural Science Foundation of China (NSFC projects 21774067 and 21374052). C. T. acknowledges the support from K. C. Wong Magna Fund in Ningbo University.

References

1 W. L. Chen, R. Cordero, H. Tran and C. K. Ober, *Macromolecules*, 2017, **50**, 4089.
2 A. Wittemann, B. Haupte and M. Ballauff, *Phys. Chem. Chem. Phys.*, 2003, **5**, 1671.
3 D. H. Napper, *Polymer Stabilization of Colloidal Dispersions*, Academic Press, New York, 1983.
4 M. P. Weir, S. Y. Heriot, S. J. Martin, A. J. Parnell, S. A. Holt, J. R. P. Webster and R. A. L. Jones, *Langmuir*, 2011, **27**, 11000.
5 G. J. Fleer, M. A. Cohen Stuart, J. M. H. M. Scheutjens, T. Cosgrove and B. Vincent, *Polymers At Interfaces*, Chapman & Hall, London, 1993.
6 S. T. Milner, T. A. Witten and M. E. Cates, *Macromolecules*, 1988, **21**, 2610–2619.
7 A. Halperin, M. Tirrell and T. P. Lodge, *Adv. Polym. Sci.*, 1991, **100**, 31–71.
8 I. Szleifer and M. A. Carignano, *Adv. Chem. Phys.*, 1996, **94**, 165.
9 S. Das, M. Banik, G. Chen, S. Sinha and R. Mukherjee, *Soft Matter*, 2015, **11**, 8550–8583.
10 A. Naji, C. Seidel and R. R. Netz, *Adv. Polym. Sci.*, 2006, **198**, 149–183.
11 O. V. Borisov, E. B. Zhulina and T. M. Birshtein, *Macromolecules*, 1994, **27**, 4795–4803.
12 R. R. Netz and D. Andelman, *Phys. Rep.*, 2003, **380**, 1.
13 P. Pincus, *Macromolecules*, 1991, **24**, 2912.
14 R. Israels, F. A. M. Leermakers, G. J. Fleer and E. B. Zhulina, *Macromolecules*, 1994, **27**, 3249–3261.
15 V. A. Pryamitsyn, F. A. M. Leermakers and E. B. Zhulina, *Macromolecules*, 1997, **30**, 584–589.
16 N. V. Brilliantov, Y. A. Budkov and C. Seidel, *Phys. Rev. E*, 2016, **93**, 032505.
17 E. B. Zhulina, T. M. Birshtein and O. V. Borisov, *Macromolecules*, 1995, **28**, 1491–1499.
18 P. Romiszowski. and A. Sikorski, *J. Chem. Inf. Comput. Sci.*, 2004, **44**, 393–398.
19 A. A. Polotsky, T. Gillich, O. V. Borisov, F. A. M. Leermakers, M. Textor and T. M. Birshtein, *Macromolecules*, 2010, **43**, 9555.
20 A. A. Polotsky, F. A. M. Leermakers, E. B. Zhulina and T. M. Birshtein, *Macromolecules*, 2012, **45**, 7260–7273.
21 H. Merlitz, C. X. Wu and J. U. Sommer, *Macromolecules*, 2011, **44**, 7043.

22 H. Merlitz, W. Cui, C. X. Wu and J. U. Sommer, *Macromolecules*, 2013, **46**, 1248.
23 C. W. Li, H. Merlitz, C. X. Wu and J. U. Sommer, *Polymer*, 2016, **98**, 437.
24 O. V. Borisov, A. A. Polotsky, O. V. Rud, E. B. Zhulina, F. A. M. Leermakers and T. M. Birshtein, *Soft Matter*, 2014, **10**, 2093.
25 E. B. Zhulina, V. M. Amoskov, A. A. Polotsky and T. M. Birshtein, *Polymer*, 2014, **55**, 5160.
26 O. V. Borisov, E. B. Zhulina, A. A. Polotsky, F. A. M. Leermakers and T. M. Birshtein, *Macromolecules*, 2014, **47**, 6932.
27 E. B. Zhulina, F. A. M. Leermakers and O. V. Borisov, *Langmuir*, 2015, **31**, 6514.
28 W. Cui, C. F. Su, H. Merlitz, C. X. Wu and J. U. Sommer, *Macromolecules*, 2014, **47**, 3645.
29 O. V. Borisov and E. B. Zhulina, *Macromolecules*, 2015, **48**, 1499.
30 J. S. Klos and J. U. Sommer, *Macromolecules*, 2015, **48**, 1179.
31 K. Miliou, L. N. Gergidis and C. Vlahos, *J. Polym. Sci., Part B: Polym. Phys.*, 2017, **55**, 1110.
32 I. C. Yeh and M. L. Berkowitz, *J. Chem. Phys.*, 1999, **111**, 3155.
33 U. Essmann, L. Perera, M. L. Berkowitz, T. Darden, H. Lee and L. G. Pedersen, *J. Chem. Phys.*, 1999, **153**, 8577.
34 H. D. Ding, C. Duan and C. H. Tong, *J. Chem. Phys.*, 2017, **146**, 034901.
35 Y. F. Ho, T. N. Shendruk, G. W. Slater and P. Y. Hsiao, *Langmuir*, 2013, **29**, 2359–2370.
36 G. S. Grest and K. Kremer, *Phys. Rev. A: At., Mol., Opt. Phys.*, 1986, **33**, 3628–3631.
37 M. J. Stevens and K. Kremer, *J. Chem. Phys.*, 1995, **103**, 1669.
38 N. E. Jackson, B. K. Brettmann, V. Vishwanath, M. Tirrell and J. de Pablo, *ACS Macro Lett.*, 2017, **6**, 155.
39 J. F. Kolb, R. P. Joshi, S. Xiao and K. H. Schoenbach, *J. Phys. Appl. Phys.*, 2008, **41**, 234007.
40 F. Zhang, H. D. Ding, C. Duan, S. L. Zhao and C. H. Tong, *Chin. Phys. B*, 2017, **26**, 088204.
41 H. Ouyang, Z. H. Xia and J. Zhe, *Nanotechnology*, 2009, **20**, 195703.
42 H. Merlitz, C. Li, C. X. Wu and J. U. Sommer, *Soft Matter*, 2015, **11**, 5688–5696.
43 C. Tong, *J. Chem. Phys.*, 2015, **143**, 054903.
44 C. Kang, S. L. Zhao and C. Tong, *Chin. J. Polym. Sci.*, 2017, **35**, 98.
45 Our preliminary study showed that, at the same parameter settings of the ratio of Bjerrum length to monomer diameter and the amount of charge carried by each monomer as those of Y-shaped polyelectrolyte brushes in this work, charge overcompensation indeed emerges for linear polyelectrolyte brushes with chain length of 100 collapsing in external electric fields.
46 E. B. Zhulina and O. V. Borisov, *J. Chem. Phys.*, 1997, **107**, 5952.